Plant Physiology and Biochemistry 102 (2016) 115–124

Contents lists available at ScienceDirect

Plant Physiology and Biochemistry

journal homepage: www.elsevier.com/locate/plaphy

Research article

Inhibition of polyamine oxidase activity affects tumor development during the maize-*Ustilago maydis* interaction

Francisco Ignacio Jasso-Robles [a], Juan Francisco Jiménez-Bremont [b], Alicia Becerra-Flora [b], Margarita Juárez-Montiel [b], María Elisa Gonzalez [c], Fernando Luis Pieckenstain [c], Ramón Fernando García de la Cruz [d], Margarita Rodríguez-Kessler [a, *]

[a] Facultad de Ciencias, Universidad Autónoma de San Luis Potosí, Av. Dr. Salvador Nava Mtz. s/n, Zona Universitaria, C.P. 78290, San Luis Potosí, Mexico
[b] División de Biología Molecular, Instituto Potosino de Investigación Científica y Tecnológica, Camino a la Presa de San José 2055, Apartado Postal 3-74 Tangamanga, 78210, San Luis Potosí, Mexico
[c] Instituto de Investigaciones Biotecnológicas-Instituto Tecnológico de Chascomús (IIB-INTECH, UNSAM-CONICET), Chascomús, Argentina
[d] Facultad de Ciencias Químicas, Universidad Autónoma de San Luis Potosí, Av. Manuel Nava Mtz, Zona Universitaria, C.P. 78290, San Luis Potosí, Mexico

ARTICLE INFO

Article history:
Received 8 September 2015
Received in revised form
29 January 2016
Accepted 11 February 2016
Available online 16 February 2016

Keywords:
Biotic stress
Cell elongation
1,8-Diaminooctane
Hydrogen peroxide
Polyamine oxidase
Plant tumors
Ustilago maydis

ABSTRACT

Ustilago maydis is a biotrophic plant pathogenic fungus that leads to tumor development in the aerial tissues of its host, *Zea mays*. These tumors are the result of cell hypertrophy and hyperplasia, and are accompanied by the reprograming of primary and secondary metabolism of infected plants. Up to now, little is known regarding key plant actors and their role in tumor development during the interaction with *U. maydis*. Polyamines are small aliphatic amines that regulate plant growth, development and stress responses. In a previous study, we found substantial increases of polyamine levels in tumors. In the present work, we describe the maize polyamine oxidase (PAO) gene family, its contribution to hydrogen peroxide (H_2O_2) production and its possible role in tumor development induced by *U. maydis*. Histochemical analysis revealed that chlorotic lesions and maize tumors induced by *U. maydis* accumulate H_2O_2 to significant levels. Maize plants inoculated with *U. maydis* and treated with the PAO inhibitor 1,8-diaminooctane exhibit a notable reduction of H_2O_2 accumulation in infected tissues and a significant drop in PAO activity. This treatment also reduced disease symptoms in infected plants. Finally, among six maize *PAO* genes only the *ZmPAO1*, which encodes an extracellular enzyme, is up-regulated in tumors. Our data suggest that H_2O_2 produced through PA catabolism by ZmPAO1 plays an important role in tumor development during the maize-*U. maydis* interaction.

1. Introduction

Ustilago maydis is a dimorphic and host-specific Basidiomycete fungus responsible for common smut or "huitlacoche" in maize. It is a model for studies on fungal mating and DNA recombination, RNA biology, cell signaling and differentiation, and biotrophic plant–pathogen interactions (León-Ramírez et al., 2014). During the life cycle of *U. maydis* three different cellular morphologies are recognized, a saprophytic unicellular haploid yeast-like cell that reproduces by budding, dikaryotic mycelium that invades the plant host, and spherical diploid spores (teliospores) that are the result of fungal karyogamy (Banuett and Herskowitz, 1996; León-Ramírez et al., 2014). The formation of the dikaryotic mycelium, after the mating of two sexually compatible yeast-like cells, is a prerequisite for host invasion and fungal growth in maize tissues. The disease is characterized by the hyperproduction of anthocyanins, the development of chlorosis and the formation of large tumors in all the aerial parts of the plant (Banuett and Herskowitz, 1996). Disease progression can be followed on leaf blades of young maize seedlings. As soon as five days post inoculation (dpi) the appearance of small tumors more or less uniformly distributed over the leaf blade, or tumors organized in clusters, becomes evident (Banuett and Herskowitz, 1996). Tumor development is a result of cell hypertrophy and hyperplasia (Banuett and Herskowitz, 1996; Callow and Ling, 1973; Doehlemann et al., 2008). Hormones of plant and fungal

Abbreviations: dpi, days post-inoculation; DAB, 3,3-diaminobenzidine; 1,8-DO, 1,8-diaminooctane; DCHBS, 3,5-dichloro-2-hydroxybenzensulphonic acid; HRP, horseradish peroxidase; HTD, 1,7-diamino heptane; PAs, polyamines; PAO, polyamine oxidase; PMSF, phenyl-methyl-sulphonyl-fluoride; Put, putrescine; qRT-PCR, quantitative reverse-transcriptase polymerase chain reaction; Spd, spermidine; Spm, spermine; tSpm, thermospermine.

* Corresponding author.
E-mail address: mrodriguez@fc.uaslp.mx (M. Rodríguez-Kessler).

http://dx.doi.org/10.1016/j.plaphy.2016.02.019
0981-9428/

origin have been proposed to be responsible for tumor initiation, growth and elongation; nonetheless their precise role in this process is unknown (Banuett and Herskowitz, 1996; Bruce et al., 2011; Reineke et al., 2008). *U. maydis* is able to produce indole-3-acetic acid (IAA) from the amino acid tryptophan. Even though IAA produced by *U. maydis* contributes to the increases in auxin levels in infected maize tissues, it was proposed not to be important for triggering host tumor formation (Reineke et al., 2008). *U. maydis* also produces cytokinins and abscisic acid (ABA) (Bruce et al., 2011). Both hormones accumulate in infected maize tissues and it has been suggested that they play a role in the maintenance of a sink status by infected host cells (Bruce et al., 2011). Other plant growth regulators such as polyamines (PAs) are accumulated in plant tumor-like structures induced by different fungal and bacterial pathogens, including tumors induced by *U. maydis* (Jiménez-Bremont et al., 2014; Rodríguez-Kessler et al., 2008; Walters and Shuttleton, 1985). PAs, putrescine (Put), spermidine (Spd), spermine (Spm) and thermospermine (tSpm) are small aliphatic amines essential for cell growth and development, cell cycle progression, and cell expansion and differentiation (Ortega Amaro et al., 2012; Paschalidis and Roubelakis-Angelakis, 2005; Takahashi and Kakehi, 2010). Changes in PA levels are prevalent under plant stress conditions (Jiménez-Bremont et al., 2014; Wimalasekera et al., 2011). Under biotic stress, the timeline of PA accumulation and the nature of the accumulated PA depend on the plant and microbe species involved in the interaction. Usually, PA accumulation is accompanied by PA oxidation through copper-containing amine oxidases (DAO; EC 1.4.3.6) and FAD-dependent polyamine oxidases (PAO; EC 1.5.3.3) enzymes. Plant PAOs are involved in terminal catabolism and back-conversion of higher PAs (Moschou et al., 2012). PAOs catalyzing terminal catabolism oxidize the carbon at the *endo*-side of the N^4 of Spd and Spm, generating 4-aminobutanal and N-(3-aminopropyl)-4-aminobutal, respectively; along with 1,3-diaminopropane (DAP), and hydrogen peroxide (H_2O_2) (Cona et al., 2006). Peroxisomal PAOs catalyze the sequential back-conversion of Spd and Spm oxidizing the carbon at the *exo*-side of the N^4 producing Put and Spd, respectively (Moschou et al., 2012). In plants, the production of H_2O_2 by PA oxidation has been correlated with signaling, reinforcement of plant cell walls, cellular defense and, regulation of programmed cell death during plant development and pathogen attack (Gonzalez et al., 2011; Jiménez-Bremont et al., 2014; Liszkay et al., 2004; Marina et al., 2013; Moschou et al., 2008, 2012).

In a previous study, we found that maize plants infected by *U. maydis* accumulate PAs, mainly free- and conjugated Put, in tumors induced by the fungus. The increase in PA content was accompanied by the up-regulation of *ZmADC*, *ZmSAMDC* and *ZmPAO1* genes (Rodríguez-Kessler et al., 2008). In the present study, we analyzed the role of maize polyamine oxidases during the interaction of this plant with *U. maydis*. Histochemical detection of H_2O_2 was performed in maize tissues with chlorotic lesions and tumors induced by *U. maydis*. The effect of the PAO inhibitor 1,8-diaminooctane (1,8-DO) on disease symptoms appearance, H_2O_2 and free polyamine content was also analyzed in infected plants. Finally, we analyzed the transcriptional regulation of six *ZmPAO* genes in chlorotic lesions and tumors induced by *U. maydis*. Our data suggest the H_2O_2 produced through PA degradation by plant PAO activity participates in tumor development during the maize-*U. maydis* interaction.

2. Materials and methods

2.1. U. maydis strains and growth conditions

The haploid strains, FB1 (a_1b_1) and FB2 (a_2b_2) of *U. maydis* (F. Banuett, California State University, Long Island, USA) were used. When necessary, they were recovered in YEPD liquid media (1% yeast extract, 1% peptone, 1% glucose), incubated at 28 °C for 2–3 days in an orbital shaker (150 rpm) and used as inoculum for subsequent experiments.

2.2. Growth of U. maydis in YEPD medium supplemented with 1,8-diaminooctane

Growth-rate curves of *U. maydis* strains FB1 and FB2 were obtained by culturing the fungus in YEPD liquid media supplemented with 0, 200, 300 and 400 μM of the PAO inhibitor 1,8-diaminooctane (1,8-DO, Sigma–Aldrich). Optical density at 600 nm (OD_{600}) was measured at different time points (0, 6, 12, 18, 24, 30, 36, 42, 48 and 54 h) starting with a culture at $OD_{600} = 0.2$. Cultures were incubated at 28 °C and 200 rpm.

2.3. Fuzz reaction on charcoal plates supplemented with 1,8-DO

FB1 and FB2 strains were mated in charcoal plates supplemented with 0, 200, 300 and 400 μM of 1,8-DO. *U. maydis* FB1 strain starting at a cell density of 10^6 cells/mL and a series of 10-fold dilutions were spotted (4 μL per spot) on charcoal nutrient medium and when dried, overlaid with 4 μl of the FB2 mating partner (Holliday, 1974). Plates were incubated at 28 °C and the induction of fuzz phenotype was monitored after 24, 48, 72 and 96 h. Images were taken using a Canon photographic camera and processed with Photoshop Elements software v 5.0.

2.4. Plant material

Zea mays (cv. Cacahuazintle) seeds were surface disinfected with 50% commercial sodium hypochlorite solution (6% free chlorine) for 30 min, and rinsed several times with sterile distilled water. Aseptic seeds were germinated in plastic containers and grown semi-hydroponically in plastic pots filled with a mixture of sand and agrolite (3:1) and irrigated with 0.5x Hoagland's nutrient solution. Seedlings were maintained in growth chambers under controlled conditions (16 h light/8 h dark cycle, 25 °C ± 2 °C, and 50% relative humidity).

2.5. Plant inoculation with U. maydis and 1,8-DO treatments

Six-day-old seedlings were inoculated in the leaf whorl with an *U. maydis* (FB1 + FB2) cell suspension (10^8 cells/mL) using a sterile syringe as described by Rodríguez-Kessler et al (Rodríguez-Kessler et al., 2008). Samples obtained from chlorotic lesions (5 dpi, 11-day-old seedlings) and from the tumor stage (11 dpi, 17-day-old seedlings) were transferred to liquid nitrogen and maintained at −80 °C until use for qRT-PCR analysis. At the tumor stage, leaf blade tumors (T), green areas surrounding the tumors with no signs of infection (ST), and leaf blade tissue with no disease symptoms (L) were collected. Leaf blade tissues of non-inoculated seedlings (C) were used as controls.

When necessary, maize seedlings were treated with the polyamine oxidase competitive inhibitor 1,8-DO prior to *U. maydis* inoculation. 1,8-DO is a stable diamine that can be added to the plant nutrient solution, and has been described as an effective inhibitor of maize PAO activity (Cona et al., 2004; Rodríguez et al., 2009). For this purpose, five-day-old seedlings were irrigated with 0.5x Hoagland's nutrient solution containing 0, 200, 300 and 400 μM 1,8-DO inhibitor. Then, 1,8-DO-treated and untreated maize seedlings (eight-day-old) were inoculated in the node region with a cell suspension of *U. maydis* (FB1 + FB2) strains. Nutrient solutions supplemented with the inhibitor were changed every three days. Eleven days post-inoculation plants (19-day-old) were monitored

for disease symptoms: chlorosis, anthocyanin accumulation, and tumor formation. The number of infected seedlings versus the number of infected seedlings with tumors was counted. Each biological replicate consisted of 20 seedlings per treatment, and the experiment was repeated five times with similar results. Seedlings were used for histochemical detection of H_2O_2 in inoculated and non-inoculated leaves as described below.

2.6. Histochemical determination of H_2O_2 production in inoculated tissues

The histochemical detection of H_2O_2 in *U. maydis*-inoculated and non-inoculated leaf blades of maize seedlings was performed as described by Hernández et al (Hernández et al., 2001). Samples of 19-day-old seedlings (treated as described in section 2.5) were vacuum infiltrated with a solution of 0.1 mg/mL 3,3-diaminobenzidine in 50 mM Tris-acetate buffer (pH 5.0) and, incubated at room temperature in the dark for 24 h. Then, plant material was incubated in 80% (v/v) ethanol solution for 10 min at 70 °C. Leaf blades were fixed in lactic acid:phenol:water (1:1:1, v/v). Images were taken using a Luxeo 4D Labomed Stereoscope and the PixelPro Image Analysis Software (version 2.7.0.0).

2.7. RNA isolation and qRT-PCR analysis

Total RNA was isolated from leaf blades of 17-day-old maize seedlings inoculated or non-inoculated with *U. maydis* (see Section 2.5) using the TRIzol® reagent (Invitrogen). After RNA extraction, DNase I (Invitrogen) treatments and first strand cDNA synthesis were performed following previously reported protocols (Rodríguez-Kessler et al., 2008). The expression level of *ZmPAO1-6* genes was estimated by qRT-PCR using the SsoAdvanced™ Universal SYBR® Green Supermix protocol (BioRad). The oligonucleotides used to amplify each *ZmPAO* gene are listed in Suppl. Table 1. qPCR thermal cycling conditions consisted of 40 PCR cycles of 10 s at 95 °C (denature) and 30 s at 60 °C (anneal/extend). Melting curves were performed starting at 65 °C and gradually increasing the temperature every 0.5 °C up to 95 °C. The cycle number at threshold (Ct value) was used for calculations of relative mRNA expression levels. The Ct value of each *ZmPAO* target gene was normalized by subtraction of the Ct value from the maize *actin 1* (*MAc1*; GenBank J01238) gene. The fold change in gene expression relative to control samples (leaf blades of non-inoculated maize plants) was calculated using the $2^{-\Delta\Delta Ct}$ method (Livak and Schmittgen, 2001). For each sample, three biological replicates were analyzed with their respective technical replicates.

2.8. Determination of PAO enzymatic activity

Plant material was ground to a fine powder and 200 mg of each sample were homogenized in 1 mL of 0.2 M potassium phosphate buffer (pH 6.5; tissue to buffer ratio 1/5, w/v) containing 1 mM phenyl-methyl-sulphonyl-fluoride (PMSF). After centrifugation, the supernatants were used for the determination of total protein concentration and PAO activity.

PAO activity was determined spectrophotometrically from leaf extracts by monitoring the formation of a pink adduct ($\varepsilon_{515} = 2.6 \times 10^4\ M^{-1}\ cm^{-1}$). The reaction mixture contained 0.2 M potassium phosphate buffer (pH 6.5), 0.06 mg horseradish peroxidase (HRP), 100 μM 4-aminoantipyrine, 1 mM 3,5-dichloro-2-hydroxybenzensulphonic acid (DCHBS) in 0.1 mL total volume, as described by Rodríguez et al (Rodríguez et al., 2009). The reaction was started by adding 2 μL of 2 mM Spd or Spm as the substrates and incubated for 2 min at 30 °C. PAO activity was expressed as nKat/mg protein. Total protein was determined by the Bradford method using bovine serum albumin as the reference standard (Bradford, 1976).

2.9. Determination of polyamine content

Free polyamine (Put, Spd and Spm) content was estimated from 19-day-old plants inoculated with *U. maydis* and treated with 0, 200, 300 and 400 μM of 1,8-DO inhibitor. Fresh plant material (300 mg) was extracted with 1 mL of 5% (v/v) perchloric acid at 4 °C. Following overnight incubation and centrifugation, 200 μL of the supernatants were dansylated in a mixture containing 200 μL of saturated Na_2CO_3, 200 μL dansylchloride (5 mg mL^{-1} acetone) and 6 μL of 100 mM 1,7-diamino heptane (HTD) as internal standard. The mixture was incubated overnight in darkness at room temperature. Reaction was stopped by adding 100 μL proline (100 mg mL^{-1}) and dansylated PAs were extracted with 400 μL toluene. The organic phase was vacuum-evaporated and dansylated PAs were dissolved in 25 μL acetonitrile and analyzed by reverse phase HPCL (Marcé et al., 1995). One-way-ANOVA and Dunnett's multiple comparison test were performed to assess statistical significance between treatments, using GraphPad Prism 5.0b software.

2.10. In silico analysis

The amino acid sequence of putative polyamine oxidases genes from maize orthologous to the *Arabidopsis thaliana* (Fincato et al., 2011) and *Oryza sativa* PAO gene families (Ono et al., 2012) were obtained by BLAST searches against the maize genome (MaizeGDB, www.maizegdb.org) and the Phytozome (www.phytozome.net) databases. Putative *PAO* genes other than the previously described *ZmPAO1* (Cervelli et al., 2000; Cona et al., 2006; Tavladoraki et al., 1998), were named after the *A. thaliana PAOs*: *ZmPAO2*, *ZmPAO3*, *ZmPAO4*, *ZmPAO5* and *ZmPAO6*. The genomic sequence of the six maize *ZmPAO* genes was analyzed *in silico* and the genomic organization of each gene was predicted with the Spidey mRNA-to-genomic alignment program of the NCBI database (http://www.ncbi.nlm.nih.gov/IEB/Research/Ostell/Spidey) by comparing the genomic and cDNA sequences. Intron distribution pattern and intron splicing phase within exons were also derived from the aligned cDNA/genomic sequence. Promoter analysis were performed with the PlantCARE database (bioinformatics.psb.ugent.be/webtools/plantcare/html/) using 1500 bp of the sequence located upstream of the main ORF start codon of each *ZmPAO* gene. Protein sequence alignments were performed using the Clustal W program, and the Needleman-Wunsch (global) and Smith-Waterman (local) pairwise alignment programs at the EBI (European Bioinformatics Institute, Cambridge, UK; http://www.ebi.ac.uk) database. Prediction of protein sorting signals and localization sites in amino acid sequences was performed with the PSORT prediction server (http://psort.hgc.jp/form.html).

2.11. Phylogenetic analysis

A phylogenetic tree that clustered the ZmPAO proteins with orthologous PAOs of other plant species was constructed by the Maximum Likelihood method using the MEGA6 program (Tamura et al., 2013). The following PAO amino acid sequences: CsPAO1 (*Citrus sinensis*, Phytozome accession no. Cs7g02060.1), CsPAO2 (Cs7g18840.2), CsPAO3 (Cs6g15870.1), CsPAO4 (Cs4g14150.1), CsPAO5 (Cs7g23790.1), CsPAO6 (Cs7g23670.1), AtPAO1-AtPAO5 (*A. thaliana*), ZmPAO1-ZmPAO6 (*Z. mays*), and OsPAO1-OsPAO6 (*O. sativa*) were aligned using MUSCLE version 4.0 (Edgar, 2004), of the EBI database using default values. The accession numbers of *A. thaliana*, *Z. mays* and *O. sativa* PAOs are indicated in Table 1. The

aligned sequences were subjected to re-sampling with replacement (1000 bootstrap) using the phylogeny tools of the MEGA6 program with default values. The amine oxidase of *Chlamydomonas reinhardtii* (CrFMS1, GenBank accession no. EDO99988.1) was used as an outgroup.

3. Results

3.1. H_2O_2 accumulation derived from PAO activity is necessary for tumor induction

The production of H_2O_2 in maize tissues infected with *U. maydis* was detected in situ after infiltration with 3,3-diaminobenzidine (DAB; Fig. 1). In comparison to control non-inoculated leaves (Fig. 1A) maize tumors show intense brown staining (Fig. 1B), indicating increased H_2O_2 production in the infected tissues. Control treatments were performed in the presence of ascorbic acid (Fig. 1C, D).

In order to determine whether H_2O_2 accumulation is due to increased PA catabolism by ZmPAOs in tumors, maize plants were treated with increasing concentrations (0, 200, 300 and 400 μM) of the competitive PAO inhibitor 1,8-diaminooctane (1,8-DO), prior to *U. maydis* inoculation. 1,8-DO is an effective inhibitor of maize PAO activity *in vivo*, is water soluble and can be easily added to the plant nutrient solution (Rodríguez et al., 2009). Under our experimental conditions, *U. maydis* was able to infect maize plants even under the highest 1,8-DO concentration; nevertheless, the number of plants with disease symptoms was reduced (Fig. 2). At the naked eye, the size of the tumors was notably reduced in a dose dependent manner, being more evident at 400 μM 1,8-DO (Suppl. Fig. 1). The inhibitor was also responsible for a reduction in leaf blade elongation, an effect previously described by Rodríguez et al (Rodríguez et al., 2009).

DAB staining revealed a notable decline in H_2O_2 accumulation in infected tissues of plants treated with 1,8-DO (Fig. 3A–D). In this way, tumors of leaf blade tissues treated with 300 and 400 μM 1,8-DO (Fig. 3C–D, respectively) exhibited a remarkable reduction in DAB staining as compared to tumors developed in plants not treated with 1,8-DO (Fig. 3A). Diminution in H_2O_2 production in these tissues correlated with a decay in PAO activity (Fig. 3E), and with a reduction of infected tissues with tumors. In addition, changes in free PA levels were observed in tumors of plants treated with 1,8-DO in comparison to tumors developed in plants not treated with the inhibitor. A significant decrease in Put level (ca. 40%) was observed using 400 μM 1,8-DO (Fig. 3F). On the other hand, the application of the inhibitor caused a two-fold increase in Spd and Spm levels; this effect was achieved with 200 μM 1,8-DO for Spd, and 400 μM 1,8-DO for Spm (Fig. 3F).

Furthermore, the effect of 1,8-DO was tested on the growth rate and the mating capacity of *U. maydis* FB1 and FB2 strains, bearing in mind that the fusion of sexually compatible strains is a limiting step in *U. maydis* pathogenic development. None of the 1,8-DO concentrations inhibited growth of FB1 and FB2 strains in YEPD liquid medium (Suppl. Fig. 2A, B). Moreover, the inhibitor exerted no negative effect on the mating capacity of compatible FB1 and FB2 strains on charcoal plates (Suppl. Fig. 2C). Fuzzy mycelia were observed even at the highest 1,8-DO concentration and in the last serial dilution after 72 h of incubation. These results showed that the PAO inhibitor 1,8-DO does not affect *U. maydis* growth, mating and filamentous growth after mating under the experimental conditions of this work.

3.2. Expression levels of ZmPAO genes in the maize-U. maydis interaction

To further characterize the role of polyamine oxidases in the maize-*U. maydis* interaction, the expression pattern of *ZmPAO* genes in chlorotic lesions and tumors was analyzed. For this purpose, BLAST analysis and keyword searches were performed in maize genome (MaizeGDB) and Phytozome databases to identify *ZmPAO* gene sequences. We found that the maize *ZmPAO* gene family is composed of six members (Table 1), which are orthologous to the well-described *A. thaliana* (*AtPAO1* to *AtPAO5*) and *O. sativa* (*OsPAO1* to *OsPAO7*) genes (Fincato et al., 2011; Ono et al., 2012). As expected, the ZmPAOs share a higher protein sequence identity with the rice PAOs (Table 1). The maize ZmPAO2, -3, and -4 enzymes show the characteristic [C/A/**S**/P]-[K/**R**]-[I/**L**/M]-motif of the peroxisome targeting signal (PST1) in their C-termini (Reumann et al., 2004), and are related to the Arabidopsis and rice peroxisomal enzymes (Suppl. Table 2; Suppl. Fig. 3A) (Ono et al., 2012; Takahashi et al., 2010). ZmPAO6 is orthologous to the rice OsPAO4 (89.7% amino acid sequence identity). In OsPAO4, a different signature (CRT sequence) for peroxisomal targeting was identified in the C-terminal region; in this sequence leucine or methionine were substituted by threonine (Ono et al., 2012). The ZmPAO6 protein also has the CRT sequence suggesting a peroxisomal localization for this enzyme (Suppl. Table 2; Suppl. Fig. 3A). ZmPAO5 is similar to AtPAO5 for which a cytosolic localization has been shown. Phylogenetic analysis grouped the ZmPAO proteins into three clades (Fig. 4A). ZmPAO1 belongs to clade I, ZmPAO5 to clade II and the

Table 1
Percentage of protein sequence identity between the *Zea mays*, *Arabidopsis thaliana* and *Oryza sativa* polyamine oxidases.

A. thaliana PAO genes TAIR Accession no.	*Z. mays* vs. *A. thaliana* % identity (Needle/Water)	*Z. mays* PAO genes phytozome Accession no.	*Z. mays* vs. *O. sativa* % identity (Needle/Water)	*O. sativa* PAO genes Gramene Accession no.
AtPAO1 (At5g13700)	40.8/47.3	ZmPAO1 (GRMZM2G034152)	76.8/81.6	OsPAO7 (OS09G0368500)
			67.5/81.8	OsPAO6 (OS09G0368200)
			49/73.8	OsPAO2 (OS03G0193400)
AtPAO2 (At2g43020)	70.3/72.2	ZmPAO2 (GRMZM2G000052)	91.5/91.5	OsPAO3 OS04G0623300
AtPAO3 (At3g59050)	69.2/71.5	ZmPAO3 (GRMZM2G396856)	90.3/90.3	
AtPAO4 (At1g65840)	61.6/61.6	ZmPAO4 (GRMZM2G150248)	88.5/88.5	OsPAO5 (OS04G0671300)
AtPAO5 (At4g29720)	40/40.3	ZmPAO5 (GRMZM2G035994)	78.9/80.1	OsPAO1 (OS01G0710200)
–	–	ZmPAO6 (GRMZM2G078033)	89.7/89.7	OsPAO4 (OS04G0671200)

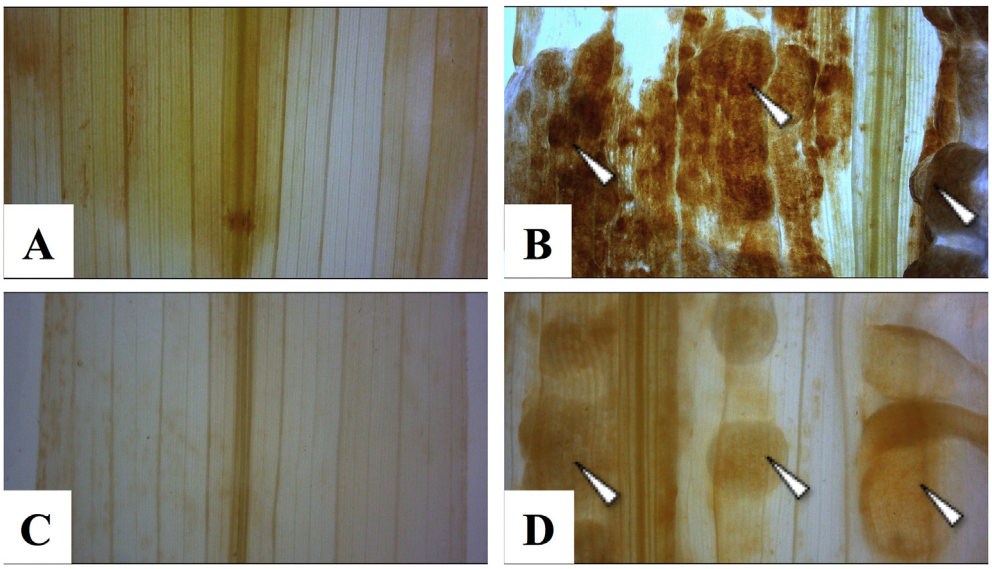

Fig. 1. Histochemical detection of H_2O_2 in maize tissues infected by *U. maydis*. Eight-day-old plants were inoculated in the node region with a cell suspension (10^8 cells/mL) of *U. maydis* FB1 × FB2 strains. Eleven days later, leaf sections were stained with 3,3-diaminobenzidine (DAB) for in situ H_2O_2 detection: (A) non-inoculated leaf blade and (B) leaf blade with tumors. DAB reagent shows H_2O_2 localization as a red-brown staining. Control leaf sections stained with DAB in the presence of ascorbic acid: (C) non-infected leaf blade and (D) leaf blade with tumors. Leaf blade maize tumors are indicated with an arrow. The experiment was repeated at least 2 times obtaining similar results.

other ZmPAOs (2, -3, -4 and −6) were assigned to clade III. Besides, the genomic organization of the *ZmPAO* genes was examined. The number of coding exons found in each gene is as follows: one (*ZmPAO5*), eight (*ZmPAO*1) and ten (*ZmPAO2*, *-3*, *-4*, and *-6*) (Fig. 4B; Suppl. Table 2).

qRT-PCR analyses of the *ZmPAO1-6* genes showed that at early stages of disease development (tissues with chlorotic lesions and anthocyanin accumulation), all *ZmPAO* genes were down-regulated (Fig. 5A). At the tumor stage, only the *ZmPAO1* gene was up-regulated, in agreement with previous findings (Rodríguez-Kessler et al., 2008). In the asymptomatic green areas that surrounded the tumors (ST) most *ZmPAO* genes were repressed (Fig. 5A). The above-mentioned results suggest that in maize tumors induced by *U. maydis*, the transcription of the *ZmPAO1* gene, which encodes an extracellular oxidase, might be responsible for the increased PAO activity in tumors and H_2O_2 production through PA catabolism.

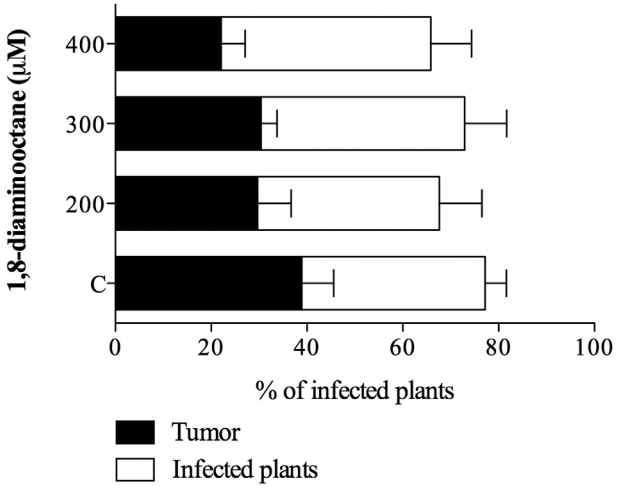

Fig. 2. Effect of 1,8-diaminooactane on disease symptoms of maize plants infected with *U. maydis*. Five-day-old maize plants grown under semi-hydroponic conditions were treated with increasing concentrations of 1,8-diaminooctane: 0, 200, 300 and 400 μM. Three days later plants were inoculated in the node region with *U. maydis*. Total bar length indicates the percentage of infected plants. The white section of each bar shows the percentage of plants that exhibited disease symptoms such as chlorosis or anthocyanin accumulation but no tumor development. The black section of each bar indicates the percentage of plants with tumors. Symptoms were scored eleven dpi. Each treatment was performed using 20 maize seedlings. The experiment was repeated five times obtaining similar results. Data are means ± SE.

In addition, the organ-specific expression of the *ZmPAO* genes was examined in leaves, stem and roots of 15-day-old maize seedlings. The relative expression level of each *ZmPAO* gene was normalized to its expression in leaves. All the six *ZmPAO* genes were expressed in the different tissues analyzed (Fig. 5B). The *ZmPAO1* gene was highly expressed in stems, as compared to other plant organs. *ZmPAO4* and *ZmPAO6* transcripts were more abundant in stem and roots than in leaves. The *ZmPAO5* gene was expressed to a similar extent in all organs analyzed. *ZmPAO2* and *-3* genes showed low expression levels in roots (Fig. 5A).

4. Discussion

Polyamine catabolism in plants mediated by flavin-containing polyamine oxidases (PAOs) contribute to the control of many important physiological processes such as defense responses to biotic and abiotic stress (Angelini et al., 2010; Cona et al., 2006; Kusano et al., 2015). PAO activity is responsible for fine-tuning cellular PA levels with the concomitant generation of important signaling molecules, such as hydrogen peroxide (H_2O_2). In the present work, we studied *ZmPAO1-6* expression levels, and the contribution of ZmPAO activity to H_2O_2 production in tumors in the maize-*U. maydis* pathosystem.

Plant tumors induced by bacterial and fungal pathogens are accompanied by cell reprogramming leading to cell hypertrophy and hiperplasia. Hormonal pathways are responsible for some of the morphogenetic changes observed in the tumor cells, giving importance to cytokinins, auxins, ABA, ethylene and other plant growth regulators such as PAs (Bruce et al., 2011; Jiménez-Bremont et al., 2014; Nassem et al., 2014; Reineke et al., 2008; Veselov et al., 2013). The maize-*U. maydis* interaction is an excellent model for the

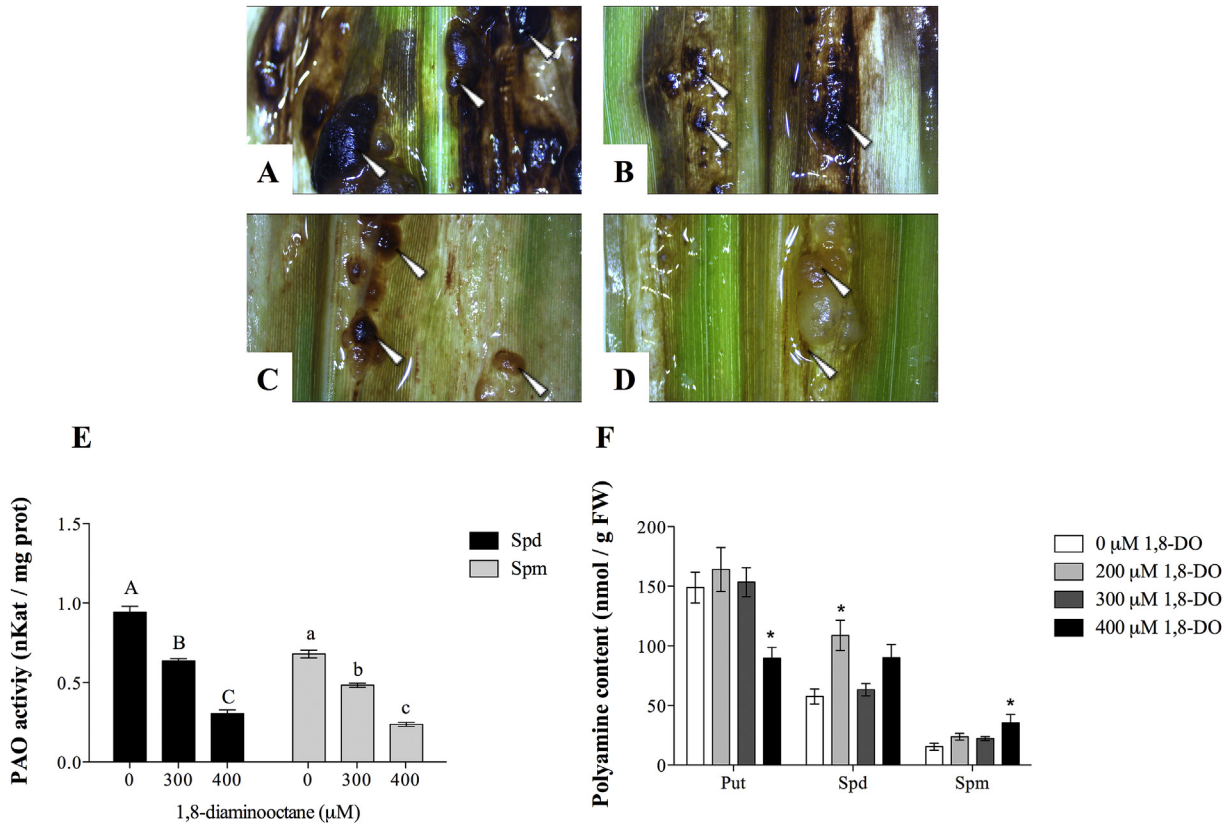

Fig. 3. Effect of 1,8-diaminooactane on H_2O_2 production and PAO activity in maize tumors induced by *Ustilago maydis*. Five-day-old maize plants grown under semi-hydroponic conditions were treated with increasing concentrations of 1,8-diaminooctane: (A) 0, (B) 200, (C) 300 and (D) 400 μM. Three days later plants were inoculated in the node region with a cell suspension (10^8 cells/mL) of *U. maydis* FB1 × FB2 strains. Seven days after inoculation, leaf sections of infected plants were stained with 3,3-diaminobenzidine for in situ H_2O_2 detection. Arrows show H_2O_2 brown staining in leaf blade maize tumors. The experiment was repeated 2 times obtaining similar results. (E) Seven days after inoculation, PAO activity of infected maize plants previously treated with 1,8-DO was measured using Spd and Spm as substrates. Inoculated plants that were not treated with 1,8-DO were used as controls. Data are means ± SE (n = 6) of a single representative experiment from two replicate experiments. Different letters indicate significant differences between samples using the same substrate (Spd or Spm) according to Two-way ANOVA at $P < 0.05$. (F) Free polyamine (Put, Spd and Spm) content of infected maize plants treated with 0, 200, 300 and 400 μM 1,8-DO. Data are means ± SE (n = 3) of a single representative experiment from two replicate experiments. Asterisks (*) indicate values that differ at $P < 0.05$ between 1,8-DO treated and untreated (control) samples according to Dunnett's multiple comparison test.

understanding of plant cell reprogramming leading to tumor development (Bruce et al., 2011). In relation to the role of PAs in tumor formation, high levels of free and conjugated Put are accumulated in maize leaf blades infected with *U. maydis*, from the onset of the development of chlorotic lesions through the establishment of tumors (Rodríguez-Kessler et al., 2008; Rodríguez-Kessler and Jiménez-Bremont, 2009). Thus, it can be hypothesized that high levels of Put are important for the cellular processes (cell division and elongation) that lead to tumor development. Herein, we detected a decrease in *ZmPAO* transcript levels in chlorotic lesions (Fig. 5A), which suggests that the important increase in PA levels previously reported (Rodríguez-Kessler and Jiménez-Bremont, 2009) at this stage of disease development is not only due to an enhancement in PA synthesis, but also to the down-regulation of PA catabolism. Conversely, in tumors induced during later stages of leaf infection by *U. maydis*, PAO activity was found to play an important role in H_2O_2 production. The contribution of PAO activity to H_2O_2 production was tested using 1,8-DO, a compound that has been previously demonstrated to act as a competitive inhibitor of maize PAO. 1,8-DO has been shown to exert PAO inhibition through a high affinity interaction with the U-shaped catalytic tunnel of the ZmPAO1 enzyme (K_i value of 3.0×10^{-7}) and is a valuable research tool for studies on plant PAOs (Cona et al., 2004; Rodríguez et al., 2009). The dramatic reduction of H_2O_2 accumulation in tumors developed on plants treated with increasing 1,8-DO concentrations detected in the present work, as well as the concomitant drop in PAO activity (Fig. 3), support the view that PAO activity strongly contribute to H_2O_2 accumulation under these conditions. The increment in free Spm level (2-fold) is also consistent with the low PAO activity in tumors of plants treated with 400 μM 1,8-DO. Taking into account that *ZmPAO1* was the only PAO gene whose expression was increased in tumors (Fig. 5A), the drop in PAO activity caused by 1,8-DO in this tissue could be related to the specific inhibition of this PAO isoform.

It is also worth to point out that the 1,8-DO inhibitor was found not to affect *U. maydis* growth, mating and filamentous growth after mating (Suppl. Fig. 2). Moreover, *U. maydis pao* mutants are still able to undergo mating and to accomplish yeast-to-hypha transitions (Valdéz-Santiago et al., 2010).

In maize tumors, a balance between PA synthesis and catabolism may be involved in the accumulation of Put and the maintenance of Spd and Spm levels (Rodríguez-Kessler et al., 2008). The high PAO activity in tumors with increased H_2O_2 accumulation could be related to cell wall enlargement, restructuring and reinforcement. ZmPAO1 is a secretory glycoprotein abundant in primary and secondary cell walls with roles in cell wall maturation and wounding healing (Angelini et al., 2008; Cona et al., 2005). Inhibition of ZmPAO1 activity with *N*-prenylagmatine affects lignin and suberin polyphenolic domain deposition in the cell wall of wounded tissues (Angelini et al., 2008). In our experiments, we

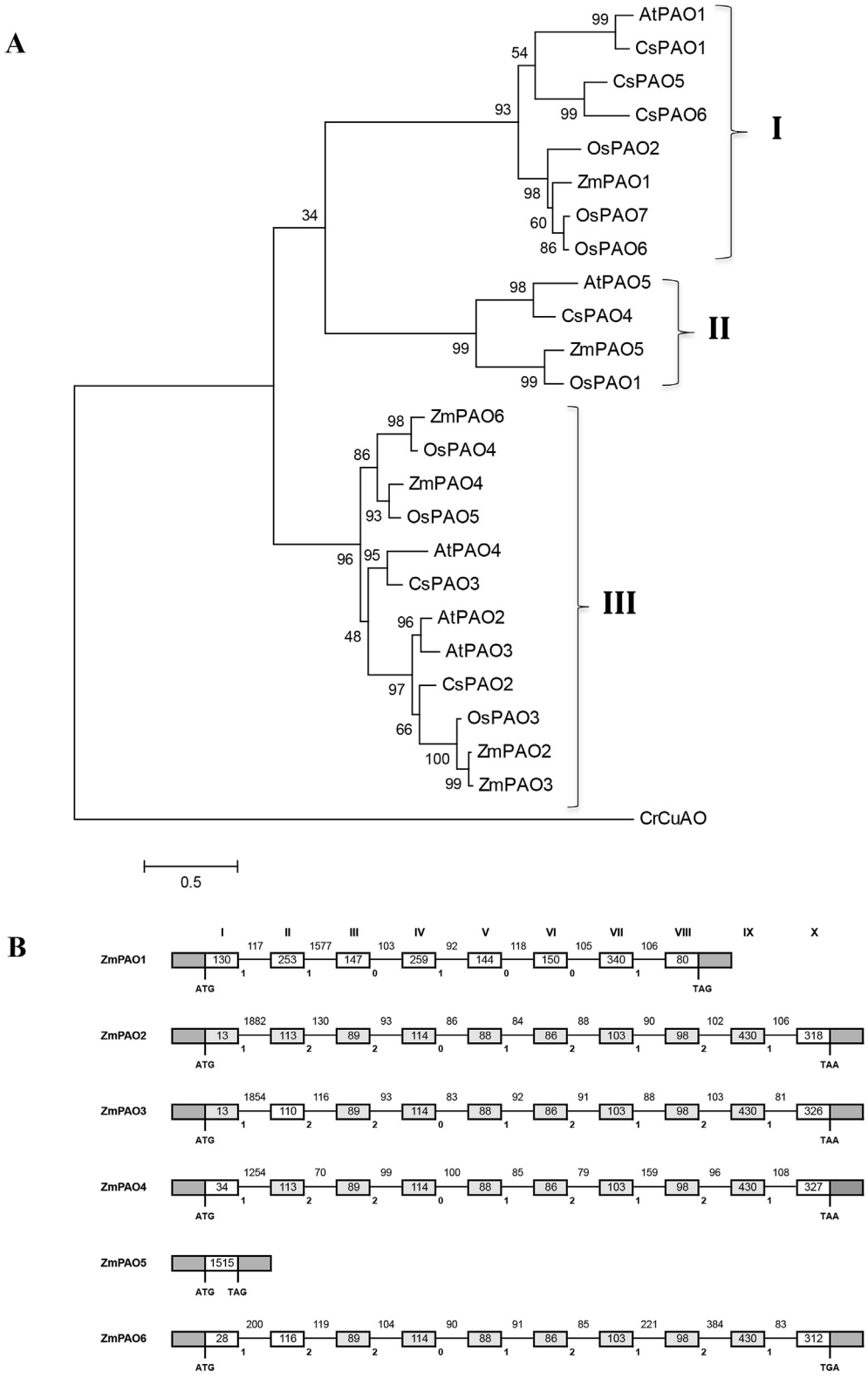

Fig. 4. Maximum Likelihood phylogenic tree of plant polyamine oxidases (A): *Z. mays* (ZmPAO1-6), *O. sativa* (OsPAO1-7), *A. thaliana* (AtPAO1-5) and *Citrus sinensis* (CsPAO1-6). The phylogenetic tree was constructed using the MEGA6 program. As outgroup the amine oxidase of *Chlamydomonas reinhardtii* (CrFMS1) was used. Genomic organization of the *ZmPAO* gene family (B). Introns are shown as solid lines and boxes represent exons. The exons of the ORF region are numbered (I to X) and exons in the UTR regions are gray shadowed. Same-length-exons are highlighted in blue. Intron phase (0, 1 or 2) is indicated below each intron.

observed that maize plants treated with 1,8-DO showed a reduction in tumor size and that leaf blades reduced in size in a 1,8-DO concentration dependent manner (Suppl. Fig. 1). This information let us to hypothesize that the inhibition of PAO activity in maize infected tissues treated with 1,8-DO reduces tumor cell elongation by affecting cell wall maturation. In support of this view, inhibition

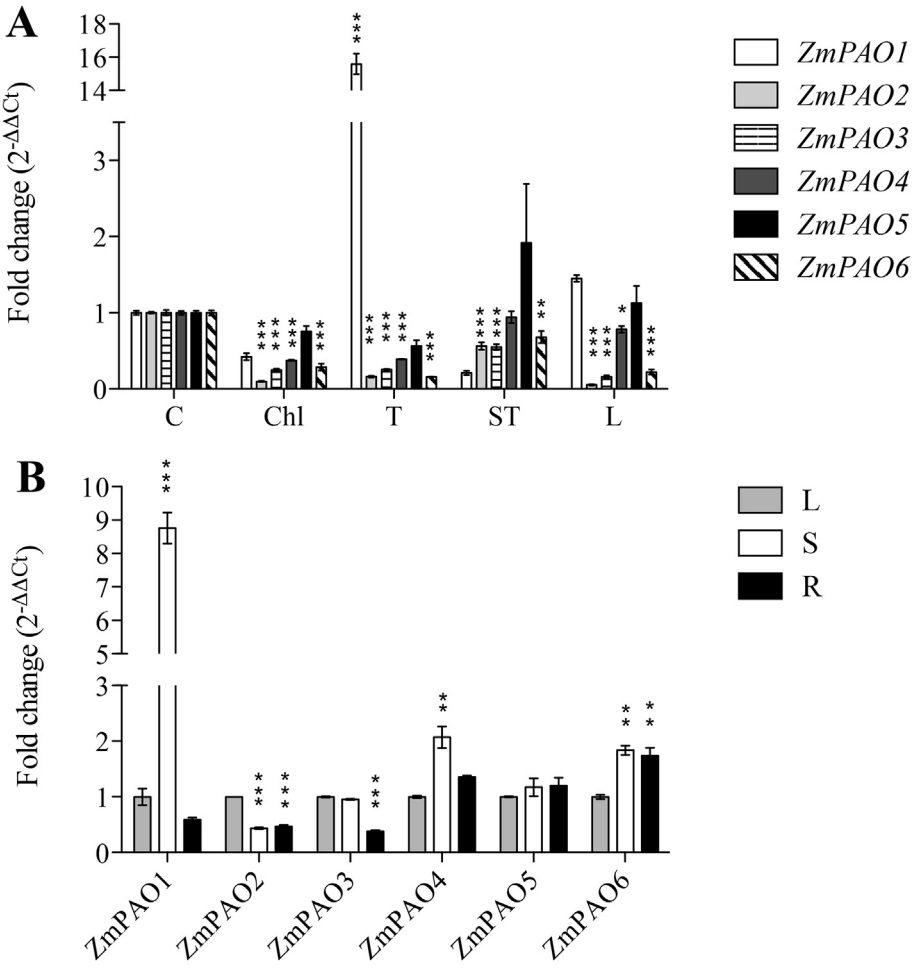

Fig. 5. Expression of *ZmPAO* genes in *Ustilago maydis*-infected plants (A), and in different maize organs (B). One microgram of total RNA from 17-day-old maize seedlings was reverse-transcribed and analyzed by qRT-PCR using SYBR green. Quantitation of *ZmPAO1-6* genes in *U. maydis*-infected plants, expressed as relative fold change of *ZmPAO* genes was calculated after normalization to the non-infected maize tissues using the comparative threshold method ($2^{-\Delta\Delta Ct}$). Control (c), chlorosis and anthocyanins (Chl), tumor (T), asymptomatic tissues that surrounded the tumors (ST) and healthy leaf (L). Quantitation of maize *ZmPAO* genes in leaves (L), stems (S) and roots (R), expressed as relative fold change of the target gene compared with its expression in a reference organ (L) was estimated with the comparative threshold method. The maize *actin-1* (GenBank J01238) gene was used as reference. Bars represent means ± SE (n = 3). Stadistical analysis was assessed by one-way ANOVA followed by Dunnett's test. *P < 0.05, **P < 0.01, ***P < 0.001.

of maize leaf blade elongation in the presence of the 1,8-DO and other PAO inhibitors has been reported (Rodríguez et al., 2009), and remarkably the authors found that PAO activity supports maize leaf elongation by the oxidation of apoplastic PAs under salt stress. Since ZmPAO1 is an apoplastic enzyme, it might be possible that tumor growth depends on Spd and Spm export to the apoplast and further production of H_2O_2 in the extracellular space. Polyamine oxidases, both apoplastic and peroxisomal, appear to be essential enzymes for cell elongation processes. In *A. thaliana*, where no apoplastic PAO enzymes have been found, the peroxisomal AtPAO3 is critical for pollen tube elongation (Wu et al., 2010) and for balancing superoxide ions (O_2^-) and H_2O_2 production (Andronis et al., 2014).

Keyword search and sequence BLAST analysis indicate that six members compose the *ZmPAO* gene family: *ZmPAO1-6* (Table 1). The maize PAO family has orthologous genes to the Arabidopsis (*AtPAO1-5*) and *O. sativa* (*OsPAO1-7*) PAO gene families, and maintains the same gene number as in the *Citrus sinensis* (*CsPAO1-6*) PAO gene family (Fincato et al., 2011; Ono et al., 2012; Wang and Liu, 2015). Phylogenetic analysis grouped the ZmPAO proteins into three clades: I (ZmPAO1), II (ZmPAO5) and III (ZmPAOs 2, -3, -4 and -6). The well described ZmPAO1 (Cona et al., 2006; Tavladoraki et al., 1998) is more related to the rice OsPAO7 enzyme involved in terminal catabolism, and also to the OsPAO6 and OsPAO2 enzymes which appear to be shorter isoforms of OsPAO7 (Kusano et al., 2015; Ono et al., 2012). The ZmPAO2, -3, -4 and -6 appear to be related to the Arabidopsis and rice peroxisomal enzymes. Interestingly, *ZmPAO2*, *-3*, *-4* and *-6* genes conserve a genomic organization with ten coding exons, and the length of most of these exons is also maintained (Fig. 4). The position of introns within codons in *ZmPAO2*, *-3*, *-4*, and *-6* genes is also highly conserved: introns 1, 5, 7 and 9 lie after the first base (phase 1), introns 2, 3, 6 and 8 are located after the second nucleotide (phase 2), and only intron 4 lies between two codons (phase 0). All these together let us suggest that they were originated by gene duplication events. Finally, the *ZmPAO5* gene lacks introns in the coding regions as reported for *AtPAO5*, *OsPAO1* and *CsPAO4* (Fincato et al., 2011; Ono et al., 2012; Wang and Liu, 2015).

Transcripts of *ZmPAO* genes were detected in leaves, stems and roots of 15-day-old maize seedlings (Fig. 5B). In Arabidopsis, the expression of the five PAO genes (*AtPAO1-5*) was observed in several tissues in 2 week-old-plantlets (Takahashi et al., 2010). The *AtPAO4* transcript was abundant in root tissues and, *AtPAO1*, *-2*, *-3* and *-5* were highly expressed in floral organs (Takahashi et al., 2010). In maize we found *ZmPAO1* and *ZmPAO4* transcripts to be more abundant in stems than in other organs, and of *ZmPAO4* and

ZmPAO6 transcripts were more abundant in root. Besides tissue specific expression, *in silico* analysis of *ZmPAO1-6* promoters shows several regulatory elements responsive to phytohormones [auxins, gibberelins, salicylic acid, methyl jasmonate (MeJA) and ABA], and to biotic and abiotic stress (Suppl. Fig. 4A). MeJA regulatory elements (CGTCA, TGACG motifs and the G-Box) were found to be common in the promoters of *ZmPAO* genes, and accordingly MeJA positively regulates the expression of *ZmPAO1*, *-3* and *-5* genes (Suppl. Fig. 2B). *ZmPAO1* responsiveness to jasmonic acid has already been reported (Angelini et al., 2008) with an important role for *ZmPAO1* gene in wound healing events. Besides *ZmPAO1*, it might be possible that the *ZmPAO* genes could also have a role in wounding and biotic stress responses that involve MeJA signaling. Upregulation of many MeJA biosynthetic genes is shown after infection of maize plants with *U. maydis* (Doehlemann et al., 2008). This highlights the importance in regulation of ZmPAOs, mainly *ZmPAO1* expression and activity during the infection process.

5. Conclusion

Maize tumors induced by *U. maydis* accumulate H_2O_2 to significant levels, and maize polyamine oxidases, mainly *ZmPAO1* whose transcript is up-regulated in tumors, may be responsible for the increment of H_2O_2. Inhibition of maize PAOs reduces disease symptoms in leaf blades infected with *U. maydis*, possibly by affecting the cell elongation processes that leads to tumor development. We suggest that the H_2O_2 produced through PA (Spd and Spm) oxidation participates in tumor development during the maize-*U. maydis* interaction.

Author contribution

FIJ-R carried out most of the experiments, and drafted the manuscript. AB-F and MJ-M collaborated with 1,8-DO assays in *U. maydis* and general data evaluation. MEG, FLP and RFGC participated in data interpretation and critical reading of the manuscript. JFJ-B and MR-K conceived the study, participated in its design and wrote the manuscript.

Acknowledgments

This work was financially supported by CONACYT (Investigación Ciencia Básica 2011-169509), Fondo de Cooperación Bilateral México-Argentina (2012-190390), Renovación de Infraestructura (INFR-2014-01224220), and Agencia Nacional de Promoción Científica y Tecnológica (PICT 2012-1716) fundings. The authors acknowledge to MC. Israel Maruri López and MC. Guillermo Vidriales Escobar from IPICYT for his technical assistance in HPCL analyses.

Appendix A. Supplementary data

Supplementary data related to this article can be found at http://dx.doi.org/10.1016/j.plaphy.2016.02.019.

References

Andronis, E.A., Moschou, P.N., Toumi, I., Roubelakis-Angelakis, K.A., 2014. Peroxisomal polyamine oxidase and NADPH-oxidase cross-talk for ROS homeostasis which affects respiration rate in *Arabidopsis thaliana*. Front. Plant Sci. 5, 132.

Angelini, R., Tisi, A., Rea, G., Chen, M.M., Botta, M., Federico, R., Cona, A., 2008. Involvement of polyamine oxidase in wound healing. Plant Physiol. 146, 162–177.

Angelini, R., Cona, A., Federico, R., Fincato, P., Tavladoraki, P., Tisi, A., 2010. Plant amine oxidases "on the move": an update. Plant Physiol. Biochem. 48, 560–564.

Banuett, F., Herskowitz, I., 1996. Discrete developmental stages during teliospore formation in the corn smut fungus. Ustil. Maydis. Dev. 122, 2955–2976.

Bradford, M.M., 1976. Rapid and sensitive method for the quantitation of microgram quantities of protein utilizing the principle of protein dye binding. Anal. Biochem. 72, 248–254.

Bruce, S.A., Saville, S.J., Neil Emery, R.J., 2011. *Ustilago maydis* produces cytokinins and abscisic acid for potential regulation of tumor formation in maize. J. Plant Growth Regul. 30, 51–63.

Callow, J.A., Ling, I.T., 1973. Histology of neoplasms and chlorotic lesions in maize seedlings following the injection of sporidia of *Ustilago maydis* (DC) Corda. Physiol. Mol. Plant P 4, 489–490.

Cervelli, M., Tavladoraki, P., Di Angostino, S., Angelini, R., Federico, R., Mariottini, P., 2000. Isolation and characterization of three polyamine oxidase genes from *Zea mays*. Plant Physiol. Biochem. 38, 667–677.

Cona, A., Manetti, F., Leone, R., Corelli, F., Tavladoraki, P., Polticelli, F., Botta, M., 2004. Molecular basis for the binding of competitive inhibitors of maize polyamine oxidase. Biochemistry 43, 3426–3435.

Cona, A., Moreno, S., Censi, F., Federico, R., Angelini, R., 2005. Cellular re-distribution of flavin-containing polyamine oxidase in differentiating root and mesocotyl of *Zea mays* L. seedlings. Planta 221, 265–276.

Cona, A., Rea, G., Angelini, R., Federico, R., Tavladoraki, P., 2006. Functions of amine oxidases in plant development and defence. Trends Plant Sci. 10, 2277–2289.

Doehlemann, G., Wahl, R., Horst, R.J., Voll, L.M., Usandel, B., Poree, F., Stitt, M., Pons-Kühnemann, J., Sonnewald, U., Kahmman, R., Kämper, J., 2008. Reprogramming a maize plant: transcriptional and metabolic changes induced by the fungal biotroph *Ustilago maydis*. Plant J. 56, 181–195.

Edgar, R.C., 2004. MUSCLE: a multiple sequence alignment with high accuracy and high throughput. Nucl. Acids Res. 32, 1792–1797.

Fincato, P., Moschou, P.N., Spedaletti, V., Tavazza, R., Angelini, R., Federico, R., Roubelakis-Angelakis, K.A., Tavladoraki, P., 2011. Functional diversity inside the Arabidopsis polyamine oxidase gene family. J. Exp. Bot. 62, 1155–1168.

Gonzalez, M.E., Marco, F., Gómez Minguet, E., Carrasco Sorli, P., Blázquez, M.A., Carbonell, J., Ruiz, O.A., Pieckenstain, F.L., 2011. Perturbation of spermine synthase gene expression and transcript profiling provide new insights on the role of the tetraamine spermine in *Arabidopsis thaliana* defense against Pseudomonas viridiflava. Plant Physiol. 156, 2266–2277.

Hernández, J.A., Ferrer, M.A., Jiménez, A., Barceló, A.R., Sevilla, F., 2001. Antioxidant systems and $O_2^{\cdot-}/H_2O_2$ production in the apoplast of pea leaves. Its relation with salt-induced necrotic lesions in minor veins. Plant Physiol. 127, 817–831.

Holliday, R., 1974. Ustilago maydis. In: King, R.C. (Ed.), Handbook of Genetics, vol. 1. Plenum, New York, pp. 575–595.

Jiménez-Bremont, J., Marina, M., Guerrero-González, L., Rossi, F., Sánchez-Rangel, D., Rodríguez-Kessler, M., Ruíz, O., Gárriz, A., 2014. Physiological and molecular implication of plant polyamine metabolism during biotic interactions. Front. Plant Sci. 5, 1–14.

Kusano, T., Kim, D.W., Liu, T., Berberich, T., 2015. Polyamine catabolism in plants. In: Kusano, T., Suzuki, H. (Eds.), Polyamines, pp. 77–88 (Chapter 6). Springer Japan.

León-Ramírez, C., Sánchez-Arreguín, J.A., Ruiz-Herrera, J., 2014. *Ustilago maydis*, a delicacy of aztec cuisine and a model for research. Nat. Resour. 5, 256–267.

Liszkay, A., Van der Zalm, E., Schopfer, P., 2004. Production of reactive oxygen intermediates ($O_2^{\cdot-}$, H_2O_2, and $^{\bullet}OH$) by maize roots and their role in wall loosening and elongation growth. Plant Physiol. 136, 3114–3123.

Livak, K.J., Schmittgen, T.D., 2001. Analysis of relative gene expression data using real-time quantitative PCR and the $2^{-\Delta\Delta CT}$ method. Methods 25, 402–408.

Marcé, M., Brown, D.S., Capell, T., Figueras, X., Tiburcio, A.F., 1995. Rapid high performance liquid chromatographic method for the quantitation of polyamines as their dansyl derivates: application to plant and animal tissues. J. Chromatogr. B 666, 329–335.

Marina, M., Vera Sierra, F., Rambla, J.L., Gonzalez, M.E., Blázquez, M.A., Carbonell, J., Pieckenstain, F.L., Ruiz, O.A., 2013. Thermospermine catabolism increases *Arabidopsis thaliana* resistance to *Pseudomonas viridiflava*. J. Exp. Bot. 64, 1393–1402.

Moschou, P.N., Paschalidis, K.A., Delis, I.D., Andriopoulou, A.H., Lagiotis, G.D., Yakoumakis, D.I., Roubelakis-Angelakis, K.A., 2008. Spermidine exodus and oxidation in the apoplast induced by abiotic stress is responsible for H_2O_2 signatures that direct tolerance responses in tobacco. Plant Cell. 20, 1708–1724.

Moschou, N.P., Wu, J., Cona, A., Tavladoraki, P., Angelini, R., Roubelakis-Angelakis, K.A., 2012. The polyamines and their catabolic products are significant players in the turnover of nitrogenous molecules in plants. J. Exp. Bot. 63, 5003–5015.

Nassem, M., Wölfling, M., Dandekar, T., 2014. Cytokinins for immunity beyond growth, galls and green islands. Trends Plant Sci. 19, 481–484.

Ono, Y., Kim, D.W., Watanabe, K., Sasaki, A., Niitsu, M., Berberich, T., Kusano, T., Y-Takahashi, 2012. Constitutively and highly expressed *Oryza sativa* polyamine oxidases localize in peroxisomes and catalyze polyamine back conversion. Amino Acids 42, 867–876.

Ortega Amaro, M.A., Rodríguez Kessler, M., Becerra-Flora, A., Jiménez-Bremont, J.F., 2012. Modulation of Arabidopsis CYCB1 expression patterns by polyamines and salt stress. Acta Physiol. Plant. 34, 461–469.

Paschalidis, K.A., Roubelakis-Angelakis, K.A., 2005. Sites and regulation of polyamine catabolism in the tobacco plant. correlations with cell division/expansion, cell cycle progression, and vascular development. Plant physiol. 138, 2174–2184.

Reineke, G., Heinze, B., Schirawski, J., Buettner, H., Kahmann, R., Basse, C.W., 2008. Indole-3-acetic acid (IAA) biosynthesis in the smut fungus *Ustilago maydis* and its relevance for increased IAA levels in infected tissue and host tumour formation. Mol. Plant Pathol. 9, 339–355.

Reumann, S., Ma, C., Lemke, S., Babujee, L., 2004. AraPerox. A database of putative Arabidopsis proteins from plant peroxisomes. Plant Physiol. 136, 2587–2608.
Rodríguez, A.A., Maiale, S.J., Menéndez, A.B., Ruiz, O.A., 2009. Polyamine oxidase activity contributes to sustain maize leaf elongation under saline stress. J. Exp. Bot. 60, 4249–4262.
Rodríguez-Kessler, M., Ruiz, O.A., Maiale, S., Ruiz-Herrera, J., Jiménez-Bremont, J.F., 2008. Polyamine metabolism in maize tumors induced by Ustilago maydis. Plant Physiol. Biochem. 46, 805–814.
Rodríguez-Kessler, M., Jiménez-Bremont, J.F., 2009. *Ustilago maydis* induced accumulation of putrescine in maize leaves. Plant Signal Behav. 4, 310–312.
Takahashi, Y., Cong, R., Sagor, G.H.M., Niitsu, M., Berberich, T., Kusano, T., 2010. Characterization of five polyamine oxidase isoforms in *Arabidopsis thaliana*. Plant Cell Rep. 29, 955–965.
Takahashi, T., Kakehi, J.I., 2010. Polyamines: ubiquitous polycations with unique roles in growth and stress responses. Ann. Bot. 105, 1–6.
Tamura, K., Stecher, G., Peterson, D., Filipski, A., Kumar, S., 2013. MEGA6: molecular evolutionary genetics analysis version 6.0. Mol. Biol. Evol. 30, 2725–2729.
Tavladoraki, P., Schininà, M.E., Cecconi, F., Di Agostino, S., Manera, F., Rea, G., Mariottini, P., Federico, R., Angelini, R., 1998. Maize polyamine oxidase: primary structure from protein and cDNA sequencing. FEBS Lett. 426, 62–66.
Valdéz-Santiago, L., Guzmán-de-Peña, D., Ruiz-Herrera, J., 2010. Life without putrescine: disruption of the gene encoding polyamine oxidase in *Ustilago maydis odc* mutants. FEMS Yeast Res. 10, 928–940.
Veselov, D., Langhans, M., Hartung, W., Aloni, R., Feussner, I., Götz, C., Veselova, S., Schlomski, S., Dicker, C., Bächmann, K., Ullrich, C.I., 2013. Development of Agrobacterium tumefaciens C58-induced plant tumors and impact on host shoots are controlled by a cascade of jasmonic acid, auxin, cytokinin, ethylene and abscisic acid. Planta. 216, 512–522.
Walters, D.R., Shuttleton, M.A., 1985. Polyamines in the roots of turnip infected with *Plasmodiophora brassicae Wor.* New Phytol. 100, 209–214.
Wang, W., Liu, J.H., 2015. Genome-wide identification and expression analysis of the polyamine oxidase gene family in sweet orange (*Citrus sinensis*). Gene 555, 421–429.
Wimalasekera, R., Tebartz, F., Scherer, G.F.E., 2011. Polyamines, polyamine oxidases and nitric oxide in development, abiotic and biotic stresses. Plant Sci. 181, 593–603.
Wu, J., Shang, Z., Wu, J., Jiang, X., Moschou, P.N., Sun, W., Roubelakis-Angelakis, K.A., Zhang, S., 2010. Spermidine oxidase-derived H_2O_2 regulates pollen plasma membrane hyperplarization-activated Ca^{2+}-permeable channels and pollen tube growth. Plant J. 63, 1042–1053.